EFFECTS OF DOPPLER SHIFT IN SPREAD SPECTRUM ACQUISITION.

T.J.Delve, P.R.Atkins

The University of Birmingham, School of Electronic and Electrical Engineering.

1. Introduction

One of the main problem areas when using a random sequence to modulate a data sequence is that of synchronising the transmitter and receiver due to the propagation delay.

As the random sequence would normally be generated using a digital code sequencer, this uncertainty in time translates into a large uncertainty in the index of the digital code sequence. If the sequence is short enough then it is possible for the receiver to perform a cross-correlation with the received code in order to determine the relative position of the local code.

However, if an eavesdropper performs an auto-correlation on the received data it will be possible to detect the presence of the signal, therefore detecting the presence of the transmitting vessel. Thus, using a short modulating sequence will compromise the covert nature of the system. It is therefore desirable for the random sequence to be at least as long as the transmission and for the sequence to be different each time a transmission is initiated.

The requirement that the random sequence is different each time complicates the task of synchronisation. A standard technique employed in radio data communications to aid synchronisation is to prefix each message with a known start-up sequence. Thus the receiver would only require a matched filter programmed to respond to the start-up sequence. This could then be used to signal to the receiver that a transmission had been detected and to start the local random sequence in order to demodulate the data. This however is also undesirable as it allows an eavesdropper to detect and demodulate the transmitted signal.

The method of starting the code in a different position each time is to have the sequences on the transmitter and receiver synchronised in time by means of an on-board clock. This implies the code sequences are running continuously. Dixon [1] gives the duration of sequences using a code rate of 1 Mcps. (Millions of chips per second). One sequence given as an example repeats every 1.95 billion years. When using locked sequence generators for the transmitter and receiver, the problem becomes one of estimating the range of the transmitting vessel in order to obtain information to use in the demodulation process. If the range is known precisely then the starting point of the random sequence is known. If the range is unknown, then there will be some uncertainty in the starting position of the random sequence.

This paper presents a partial analysis of the problem of synchronisation time by modelling the detection process using Markov techniques. The paper analyses the case for a baseband system with a bandwidth of 2kHz and a dual integration system, see Figure 1. The paper shows that the choice of search method and detection technique are significant in determining the synchronisation time. The paper goes on to demonstrate the problems involved when one of the platforms is moving.

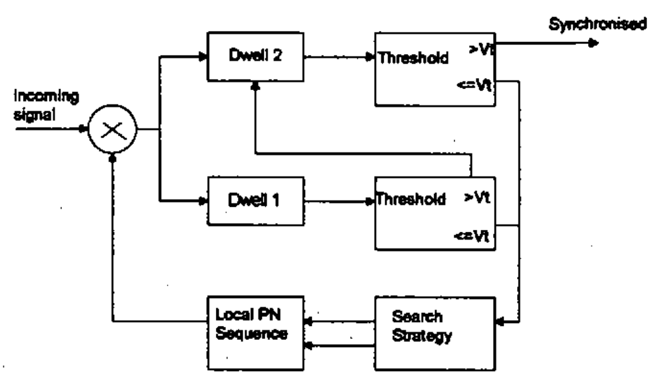

Figure 1

2. P.N. Acquisition analysis

The analysis of the synchronisation problem may be broken down into a series of detection problems. When the local code is not in phase with the received code the detection process is driven by the false alarm probability of the system. This in turn is governed by the power of the ocean noise and the power of the correlation noise. For analysis purposes, the statistics of the ocean noise are considered finite and stationary. The correlation noise is however a function of the range of the transmitting vessel. The following work will present an analysis of the synchronisation problem.

2.1 Detection and decision mechanisms

There are a number of synchronisation methods available each with its own merits. Given a known signal to detect, it can be shown that in the presence of Gaussian noise a matched filter is the optimum detector. During the synchronisation process a decision must be made as to whether the local code phase is correct. The level of any hard boundary used to make this decision will affect the system detection and false alarm probabilities. In order to understand how this decision threshold effects the synchronisation time an understanding of the detection and false alarm probabilities of the matched filter is required.

The parameters used to describe the characteristics of the synchronisation are as follows :

$\alpha(f,r)$ signal loss due to absorbtion for a given frequency f and range r;

EFFECTS OF DOPPLER SHIFT IN SPREAD SPECTRUM ACQUISITION.

$\beta(r)$ signal loss due to spreading given range r;
P_t power of the transmitted signal;
P_l power of the locally generated replica;
G gain of the receiver.

The local replica in the transmitter and receiver is denoted by $s(t)$ having power P_l. The received signal is given by :

$$s_r(t) = k \cdot s(t) \text{ where } k = \sqrt{\alpha(f,r) \cdot \beta(r) \cdot \frac{P_t}{P_l} \cdot G}$$

The two situations of interest are when the local replica is in phase with the received signal and when the replica and received signal are out of phase. For both of these cases the received noise and correlation noise will affect the detection performance. Considering this first.

The mean power obtained at the output of the matched filter caused by ocean induced input noise signal is given by:

$$P_{no} = \frac{N_0}{2}\varepsilon_s = \sigma_{no}^2$$

where ε_s is the energy of the local replica and $\frac{N_o}{2}$ is the noise density of the ocean.

The normalised correlation noise or self noise power is given by Golds approximation :

$$\sigma_{gc}^2 = \left(\frac{1}{N} - \frac{1}{N_s}\right)\left(1 + \frac{1}{N_s}\right)$$

where N = Number of chips correlated, N_s = sequence length in chips.

In order that this may be used within the analysis of a matched filter the value needs to be corrected to convert it to the real power available. The correlation noise becomes :

$$\sigma_c^2 = (kTP_l)^2 \cdot \sigma_{gc}^2$$

Where T is the observation time of the filter.

The mean noise power at the output of the correlator becomes the sum of the code noise and ocean induced output noise:

$$\sigma_o^2 = \sigma_{no}^2 + \sigma_c^2$$

EFFECTS OF DOPPLER SHIFT IN SPREAD SPECTRUM ACQUISITION.

For the case where the local replica is in phase with the received signal, the mean output, μ_o, corresponding to the signal is given by :

$$\mu_o = k \cdot \varepsilon_s$$

Recognising that $\varepsilon_s = T \cdot P_l$, the mean output becomes :

$$\mu_o = k \cdot T \cdot P_l$$

The values of μ_o and σ_o^2 can be used to determine the decision threshold to achieve the appropriate probability of detection and false alarm are respectively P_d and P_{fa}.

Given suitable functions for $\alpha(f, r)$ and $\beta(r)$ it is possible to determine the signal to noise ratio at the output of the correlator as a function of range. In this paper, the results are produced by using an attenuation function $\alpha(f, r)$, due to Coates [2] and assuming that the spreading $\beta(r)$, is spherical.

The signal-to-noise ratio at the correlator output is given by :

$$SNR_o(r) = \frac{[k(r) \cdot T \cdot P_l]^2}{\sigma_{no}^2 + \sigma_c^2}$$

The system probabilities may be determined by using either :

$$P_{fa}(r) = Q\left(\sqrt{SNR_o(r)} + Q^{-1}(P_d)\right)$$

for constant detection probability, or

$$P_d(r) = Q\left(Q^{-1}(P_{fa}) - \sqrt{SNR_o(r)}\right)$$

for constant false alarm probability.

Where:

$$Q(z) = \frac{1}{\sqrt{2\pi}} \int_z^\infty \exp\left(\frac{-\lambda^2}{2}\right) d\lambda$$

The synchronisation time may be analysed using these probabilities.

EFFECTS OF DOPPLER SHIFT IN SPREAD SPECTRUM ACQUISITION.

3. Synchronisation

3.1 Synchronisation description

The synchronisation operation may be separated into three distinct sections as follows :

1) The false alarm driven search up to the point of correct phase alignment;

2) the detection at the point of correct alignment;

3) the false alarm driven search from the cell coresponding to the correct alignment until the end of the uncertainty region corresponding to the maximum operation range.

Each of the sections requires a certain amount of time to evaluate and may be repeated depending upon the success of the detection. The synchronisation problem can be regarded as a search through a known uncertainty region for a feature that exists in cell r of a total R cells. Even when the correct cell has been reached it is possible to miss the feature due to the noise background.

The synchronisation problem is shown in figure 2.

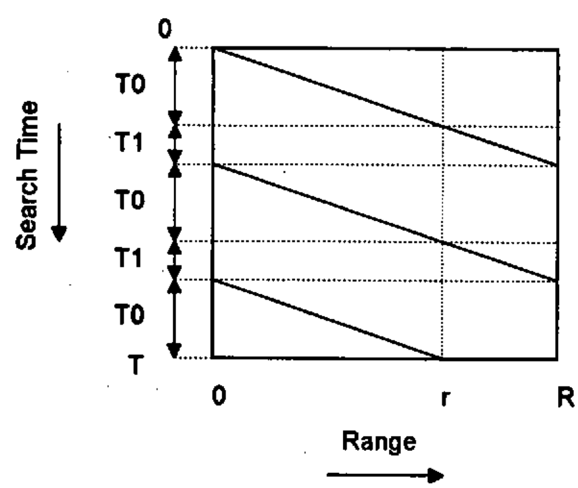

Figure 2 - Representation of the search problem.

The figure shows the search progressing from $t = 0$ moving through the uncertainty region in a linear fashion. In this example the search misses the cell at range r twice before finally making a detection at time T. The time to synchronisation in this case would be $T = 3T_0 + 2T_1$ plus

EFFECTS OF DOPPLER SHIFT IN SPREAD SPECTRUM ACQUISITION.

the time to make the decisions when the correct range cell has been reached. The object of the analysis is to derive an expression for the synchronisation time T.

3.2 Markov process analysis.

Markov analysis may be applied to a problem where the process may be separated into discrete operations. These processes may be in either continuous or discrete time. To be able to apply the analysis to the problem, the method of detection needs to be considered. The following discussion will deal with the analysis of the matched filter detector.

3.3 Flow graph representation of the detector

The list given in the previous section details the different phases of the search. The analysis of phase 1 and phase 3 is identical and will be dealt with together. The analysis will use two integrations of T_{i1} and T_{i2} seconds corresponding to the dual dwell (integration) search strategy shown in figure 1.

The figures below show the flowgraph representations of the two different search scenarios.

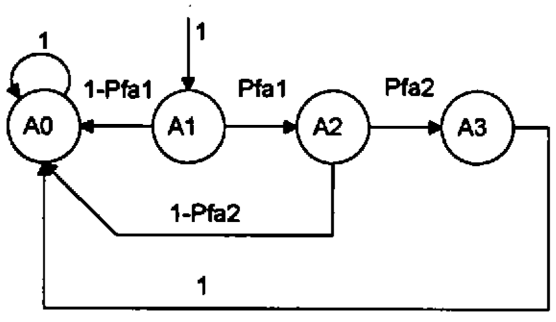

Figure 3 - Model for search of incorrect cells

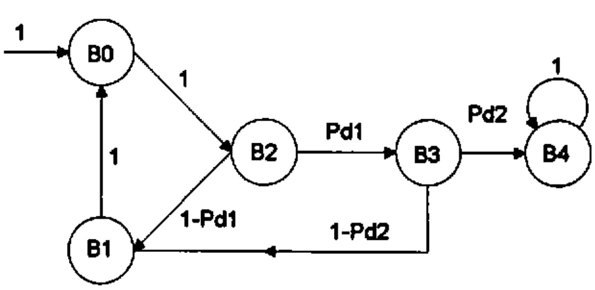

Figure 4 - Correct cell search model.

The descriptions of states in Figures 3 and 4 are given in tables 1 and 2 respectively.

State	Description	Duration
A0	Correct rejection of invalid cell	0
A1	Test invalid cell	T_{i1}
A2	Test invalid cell again	T_{i2}
A3	Penalty state for accepting incorrect cell	T_p

Table 1 - State descriptions for search of incorrect cells.

EFFECTS OF DOPPLER SHIFT IN SPREAD SPECTRUM ACQUISITION.

State	Description	Duration
B0	Represents the time taken to reach the range cell	T_0
B1	Represents the penalty time for missing the range cell	T_1
B2	Represents the test of the range cell	T_{i1}
B3	Represents the second test of the range cell	T_{i2}
B4	Represents system synchronisation	0

Table 2 - State descriptions search of the correct cell.

The mean time to correctly reject a false cell may be found by applying Markov analysis to the flowgraph shown in figure 3. The rejection time, T_s, is found to be :

$$T_s = T_{i1} + P_{fa1} \cdot (T_{i2} + P_{fa2} \cdot T_p)$$

Applying the same analysis to figure 4, the mean time to synchronise is given by :

$$T = \frac{1}{P_{d1} \cdot P_{d2}} \cdot \{T_0 + T_{i1} + P_{d1} \cdot T_{i2} + T_1 \cdot (1 - P_{d1} \cdot P_{d2})\}$$

The penalty times T_0 and T_1 for the linear search case are given by integrating the rejection time T_s:

$$T_0 = \int_0^r T_s(x)\, dx \text{ and } T_1 = \int_r^R T_s(x)\, dx$$

The analysis problem comes from specifying the detection and false alarm probabilities, P_d and P_{fa} as these vary with range.

In Gaussian noise P_{fa} and P_d are given by the following :

$$P_{fa}(r) = Q\left(\frac{V_t}{\sigma_{no}(r)}\right) \text{ and } P_d(r) = Q\left(\frac{V_t - \mu_0(r)}{\sigma_{no}(r)}\right)$$

where V_t is the decision threshold;

μ_0 is the mean output voltage of the matched filter when synchronised;

σ_{no} is the standard deviation of the correlator output noise.

3.4 Off line synchronisation

The synchronisation analysis in this paper considers an off-line method using matched filter detection. Figure 5 below shows the storage arrangement required by the synchronisation system.

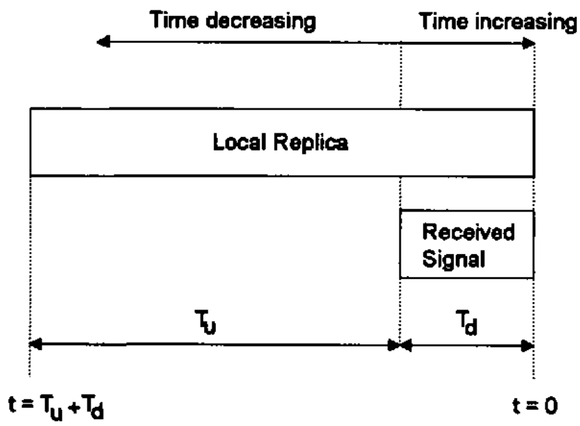

where:

T_u, the time corresponding to the maximum uncertainty in range;

T_d, the time corresponding to the maximum observation time required.

Figure 5

The value used for T_d will depend upon two factors. The first and key factor is the total time required for a single detection of a correct cell. The second factor is the mean number of times required to detect the correct cell. So, if a dual integration detector with integration times of T_1 and T_2 seconds is used in a noisy environment where the mean number of passes before detection is P, the value of T_d is given by:

$$T_d = P \cdot (T_1 + T_2)$$

The synchronisation system would then correlate the section of received code with the appropriate section of the local replica to attempt to determine the received code phase. The number of passes around a data set would depend upon the data storage capacity of the system and the mean time to synchronise. So, the synchronisation system would have to consist of a number of banks of data large enough to deal with the code phase uncertainty and the time required to synchronise.

3.5 Synchronisation results - Stationary platforms

The results of the Markov analysis are shown in figures 7 and 8. These figures are based on a signal-to-noise ratio at 20 km of -30 dB and false synchronisation penalty time of $T_p = 36$ ms. The penalty time is based upon a system proposed by Hopkins [3] which does not declare loss of synchronisation until three successive failures to detect the code. It should be noted that this time is an off-line computation time and would correspond to several seconds of real time data.

In the analysis, the integration times and the actual computation times are as shown in table 3 below. The computation times are based on estimates of Motorola DSP 96002 timings. Although not necessarily accurate, the times are of the correct order.

Integration time	Computation time
0.5 s	2 ms
1 s	5 ms
2 s	12 ms
4 s	24 ms

Table 3

Figure 8 shows a comparison of a single and dual dwell system where $T_{i1} = 0.5s$ for both and $T_{i2} = 2s$ for the dual dwell system. The figure shows that the dual dwell system outperforms the single dwell arrangement at all ranges. This is due to the fact that the second integration while increasing the overall time spent integrating reduces the number of false declarations of synchronisation, as this penalty time is larger than either of the integration periods the overall synchronisation time is reduced.

Figure 7 shows the result of two different sets of dwell times compared to that of figure 8. From the figure it can be seen that increasing either the first or second integration period has a detrimental effect upon the synchronisation time. This demonstrates the difficulty in choosing the dwell times of the system. In order that an optimum set of integration periods is used, further analysis is required particularly with respect to the signal-to-noise ratio expected.

Both figures 7 and 8 employed a linear search technique as described by figure 2. This however is not the only search strategy available. Figure 9 shows a comparison between the linear search technique and a search strategy that could be described using the methods of Polydoros and Weber [4] as a *contracting Z search*. With this technique the synchronisation system searches the start of the uncertainty region first, followed by the end and gradually moves in towards the centre. From inspection of figure 9 it can be seen that the long distance synchronisation time has been improved albeit at the expense of the short to medium distance performance.

EFFECTS OF DOPPLER SHIFT IN SPREAD SPECTRUM ACQUISITION.

4. Processing loss due to Doppler shift

In order to compute the mean synchronisation time, the Markov technique used requires knowledge of the correlator output signal-to-noise ratio. Inspection of a typical ambiguity surface shows that the correlator output drops dramatically with both increasing speed and range. Figure 10 shows a section of an ambiguity diagram for a scenario where the vessels will close on each other at speeds upto 15 knots. From the figure it can be seen that as the range moves away from zero, the correlator output drops away rapidly from its maximum value. However, as speed increases for a given range, the width of the correlation function increases. To be able to apply Markov analysis to the Doppler shifted synchronisation process, an expression is required for the mean correlator value under Doppler shifted conditions.

Previous authors have analysed the synchronisation problem when Doppler shift has become a problem. Holmes and Chen [5] and Remley [6] dealt with the Doppler shift by considering it as narrow band problem, while Cheng *et al* [7] considered using a bank of correlators each dedicated to a certain Doppler shift. This section will now develop a wideband expression for the situation where the transmitter and receiver are moving towards each other, i.e. the received signal will be compressed.

Consider the situation in figure 6 below:

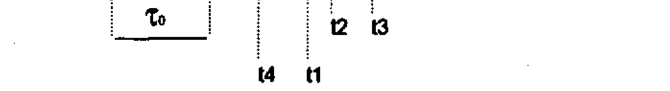

Figure 6

This depicts the two signals being correlated. Signal 1 represents the uncompressed replica at the receiver, while signal 2 represents the time shifted and time compressed received signal. (in this case signal 2 is shown as a clean unattenuated version of signal 1). The compression factor is given by:

$$d = \frac{c - V_t}{c + V_r}$$

EFFECTS OF DOPPLER SHIFT IN SPREAD SPECTRUM ACQUISITION.

where V_t is transmitter speed and V_r is receiver speed. Positive speed is considered to be when the vessel in question is moving towards the other.

So,
$$s_2(t) = s_1\left(\frac{t}{d} - \tau_0\right)$$

Where t is time, d is compression factor and τ_0 is propagation delay.

As the correlation is defined as, $R(\tau) = \int_0^T s_1(t) \cdot s_2(t+\tau)\, dt$. If we only consider the time that the two signals are known to be correlated we can see that there are in fact two stages involved in the correlation. The first stage is from time $t = 0$ through the point the replica and received signal start to come into phase, until the point at which the two signals are starting to get out of phase. The second stage starts as soon as the two signals start to get out of phase, through the point where they are completely out of phase up until the end of the correlation. To compute the mean value, we need to compute the correlated part of the signal.

From figure 6, for a particular random sequence index, n, the time the two signals are correlated during stage 1 is given by:

$$\begin{aligned} t_{c1} &= t_1 - t_2 \\ &= (n+1) \cdot T_c - n \cdot T_c \cdot d - \tau \\ &= n \cdot T_c \cdot (1-d) + T_c - \tau \end{aligned} \tag{1}$$

and during stage 2 by:

$$\begin{aligned} t_{c2} &= t_3 - t_4 \\ &= (n+1) \cdot T_c \cdot d - n \cdot T_c + \tau \\ &= T_c \cdot d + \tau - n \cdot T_c \cdot (1-d) \end{aligned} \tag{2}$$

Where T_c is the chip time.

By considering the chips at which these times start and end, the points at which each phase starts and ends are given by:

$$N_{s1} = \frac{\tau - T_c}{T_c \cdot (1-d)} + 1 \qquad N_{s2} = \frac{\tau}{T_c \cdot (1-d)}$$

$$N_{e1} = \frac{\tau}{T_c \cdot (1-d)} - 1 \qquad N_{e2} = \frac{T_c \cdot d + \tau}{T_c \cdot (1-d)} - 1$$

EFFECTS OF DOPPLER SHIFT IN SPREAD SPECTRUM ACQUISITION.

The condition on all of these being that:

$$0 \le N_{s1}, N_{e1}, N_{s2}, N_{e2} \le N_c$$

where $N_c = \frac{T}{T_c}$, the number of chips in the filter.

Given a signal $s_1(t)$ with amplitude ± 1, the correlation value of stage 1 and 2 is given respectively by:

$$R_1 = \sum_{n=N_{s1}}^{N_{e1}} t_{c1}(n) \text{ and } R_2 = \sum_{n=N_{s2}}^{N_{e2}} t_{c2}(n)$$

Using equations (1) and (2), these summations become:

$$\begin{aligned} R_1 &= \tfrac{1}{2}(N_{s1} - N_{e1} - 1) \cdot (2(\tau - T_c) - T_c \cdot (1-d) \cdot (N_{s1} + N_{e1})) \\ R_2 &= \tfrac{1}{2}(N_{s2} - N_{e2} + 1) \cdot (2(\tau - T_c) - T_c \cdot (1-d) \cdot (N_{s2} + N_{e2} + 2)) \end{aligned}$$

The final value of the correlator output is given by:

$$R = R_1 + R_2$$

This may be normalised by dividing by the filter length T.

Figures 11, 12 and 13 show the results of the calculation of the mean value compared to the actual correlator output for speeds of 3, 6 and 9 knots and the following parameters, $T_c = 1$ ms, $T = 0.512$ s, sequence length $N_s = 65535$ and an ocean noise bandwidth of $BW = 2$ kHz. The figures show that the theory and real results compare well.

Inspection of the figures shows that the peak of the correlator output shifts with increasing speed. From the graphs it can be seen that the theoretical values have followed this shift in time. Figure 15 shows the contour plot of a theoretically derived ambiguity diagram. The shift of the correlation peaks with increasing speed can clearly be seen.

An area of theory not yet completed concerns the noise generated during correlation of the Doppler shifted signal. Figure 14 shows successive correlator outputs when correlating signals with Doppler shift due to a vessel moving at 3, 6 and 9 knots. The figure shows that as speed increases, the self noise of the correlation increases. Before a complete description of the synchronisation process is available, the analysis of this noise will have to be completed.

Figure 16 shows the result of using the peak value obtained from the theory to predict the synchronisation time of the system when the correlation has not been Doppler corrected. From the figure it can be seen that as the speed increases the synchronisation time increases rapidly.

EFFECTS OF DOPPLER SHIFT IN SPREAD SPECTRUM ACQUISITION.

If the speed were sufficiently high then the system would not synchronise at all. In situations where such speeds are possible a two dimensional search would be required (that is both range and Doppler searches). An alternative to this would be to encode the transmitted signal in such away that the receiver may extract the Doppler shift from it. Figure 17 shows the results of such a signal used during a sea trial. The graph shows the radial velocity of the transmitter as it manoeuvres around a sonobouy. At $t = 0$ the vessel is approximately 4 km from the receiver. From the figure the radial velocity of the transmitter first increases, then drops to zero as the manoeuvre takes place. The speed is seen to increase from about $t = 1100$ s until the vessel passes the point of closest approach at $t = 1400$ s and continues to move away from the receiver. The problem with a signal of this sort is that the method of Doppler encoding is to create a feature in the autocorrelation of the signal. This feature can be observed to move when Doppler shifted. However, as the system is required to be covert any features present in an auto-correlation could also be seen by a hostile observer.

5. Conclusions

This paper has presented work concerned with the synchronisation of spread spectrum systems. The problem regarding stationary platforms at varying ranges has been analysed and results presented. These results show that a dual dwell (integration) synchronisation system would outperform a single dwell system when the signal-to-noise ratio was low and the penalty time was high. Results were presented showing the problem of selecting the appropriate dwell times for the system. These results showed that although an arbitrary choice of dwells was seen to work well, further analysis is required to predict the optimum value.

Consideration has been given to the problem of synchronising a wideband spread spectrum system when either the transmitter or receiver are moving. The paper has produced a set of equations that predict the mean value of a correlator output when correlating a compressed signal with an uncompressed replica. The paper showed the effect of attempting to synchronise the system with a Doppler shifted signal for various vessel speeds. From the results it was seen that at long ranges, when the detection probability is low, the detection time increases dramatically.

Further work is required on the synchronisation problem particularly in the modelling of the noise produced by a correlator under Doppler shifted conditions. A complete Markov analysis of the two dimensional search problem is required before an optimum solution is available. However, the results so far are encouraging and further analysis should yield interesting results.

Acknowledgements.

This work was funded by the Defence Research Agency (Passive Sonar Division).

EFFECTS OF DOPPLER SHIFT IN SPREAD SPECTRUM ACQUISITION.

6. References

[1] Robert C. Dixon, *'Spread Spectrum Systems (2nd Edition)'*, Wiley Interscience. Published 1984.

[2] R. W. F. Coates, *'Underwater acoustic systems'*, Macmillan New Electronics Series. Published 1990.

[3] Philip M. Hopkins, *'A unified analysis of pseudonoise synchronisation by envelope correlation'*, IEEE trans. comms. August 1977. pp 770-778.

[4] Andreas Polydoros and Charles L. Weber, *'A unified approach to serial search spread spectrum code acquisition - Part 1: General theory'*, IEEE trans. comms. May 1984. pp 550-560.

[5] J. K Holmes and C. C. Chen, *'Acquisition time performance of PN spread spectrum systems'*, IEEE trans. comms. August 1977. pp 778-783.

[6] W. R. Remley, *'Doppler dispersion effects in matched filter detection and resolution'*, Proc. of the IEEE. January 1966. pp 33-39.

[7] Unjeng Cheng *et al*, *'Spread spectrum code acquisition in the presence of Doppler shift and data modulation.'*, IEEE trans. comms. February 1990. pp 241-250.

EFFECTS OF DOPPLER SHIFT IN SPREAD SPECTRUM ACQUISITION.

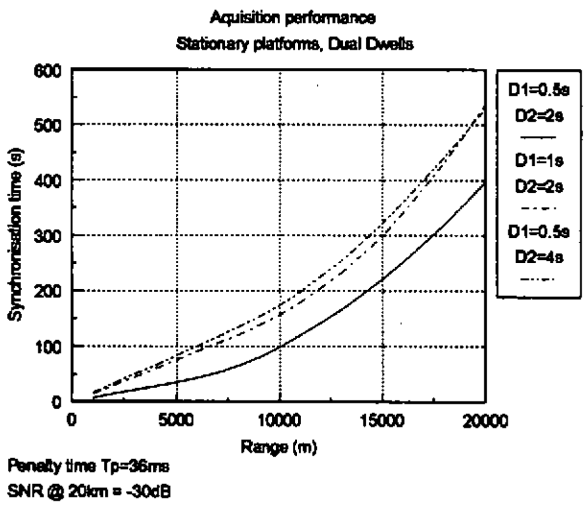

Figure 7 - Dual dwell synchronisation comparison

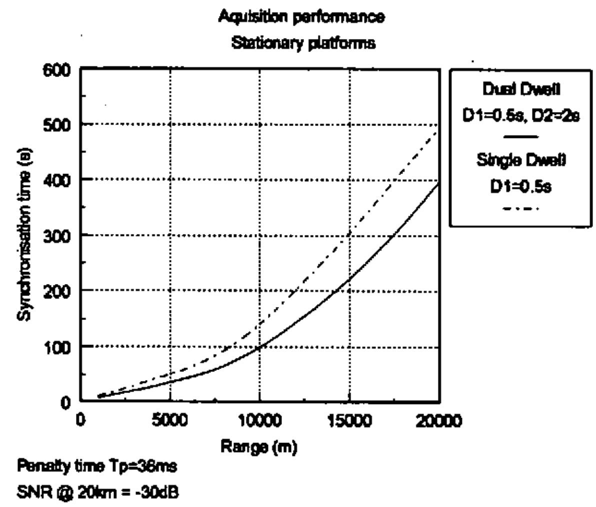

Figure 8 - Single and Dual dwell comparison

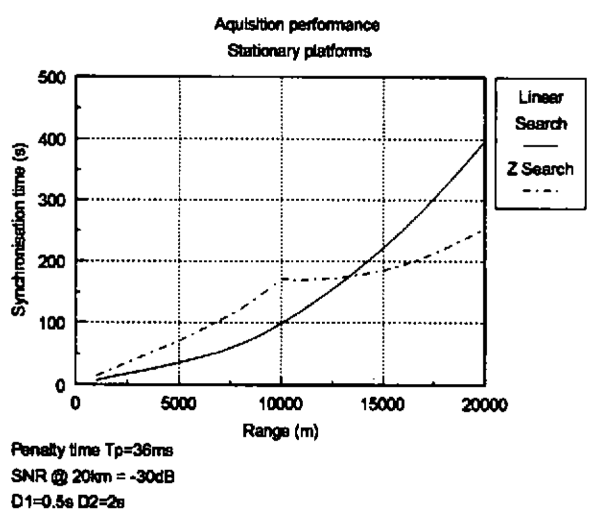

Figure 9 - Linear and Z search comparison

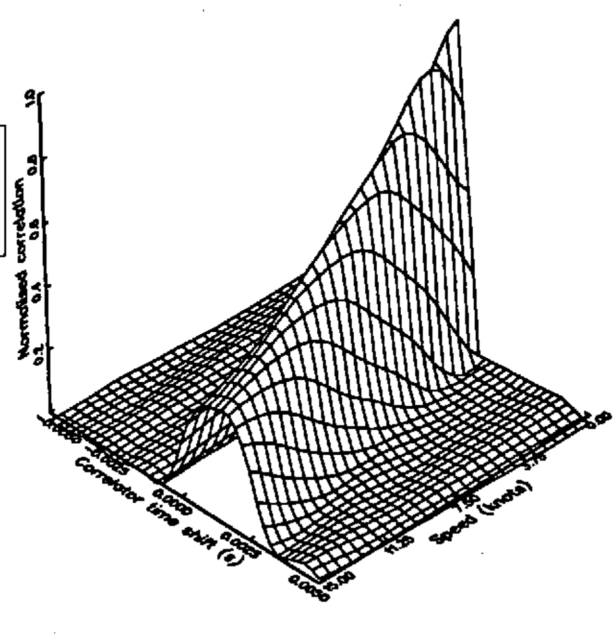

Figure 10 - Partial ambiguity diagram of a pseudo noise signal

EFFECTS OF DOPPLER SHIFT IN SPREAD SPECTRUM ACQUISITION.

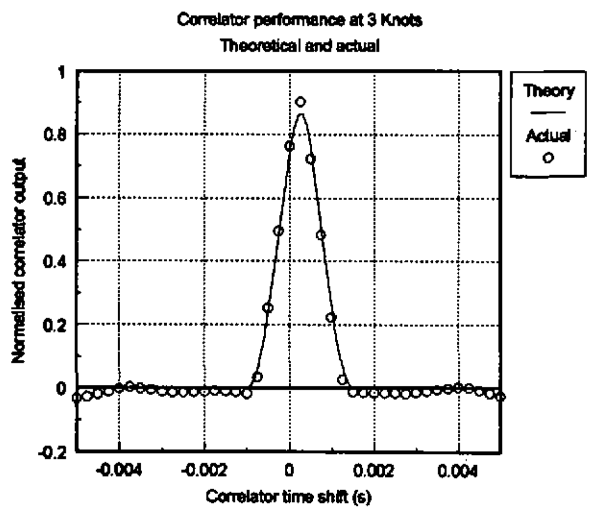

Figure 11 - Correlator output at 3 knots
Theoretical and practical

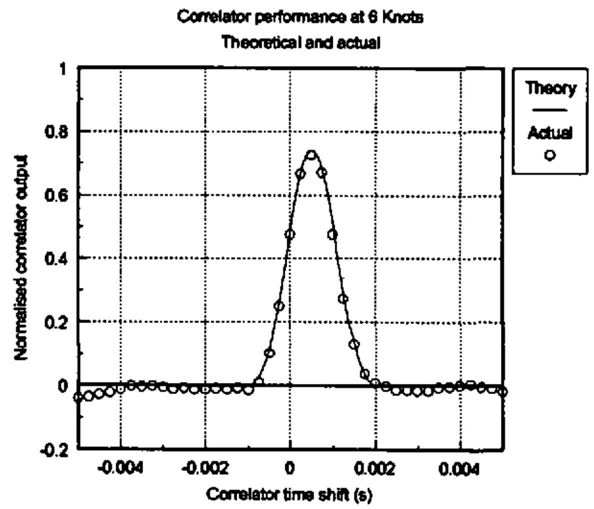

Figure 12 - Correlator output at 6 knots
Theoretical and practical

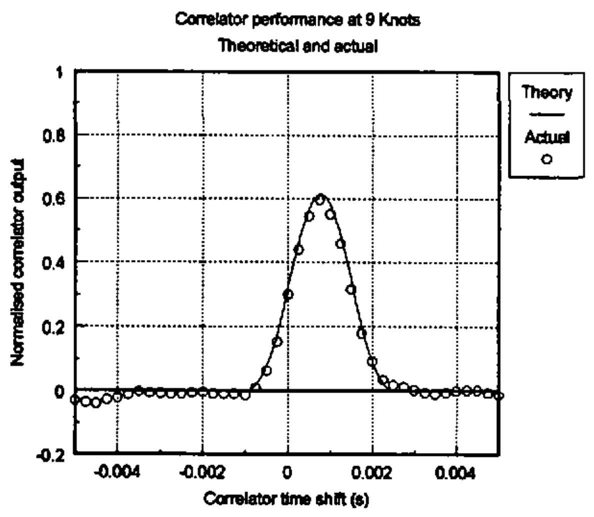

Figure 13 - Correlator output at 9 knots
Theoretical and practical

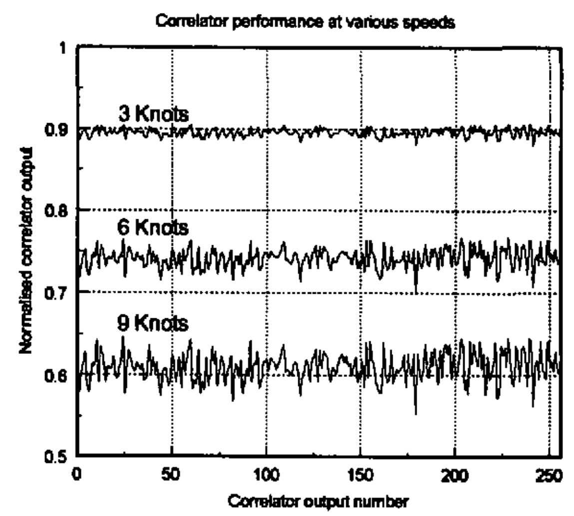

Figure 14 - Successive correlator outputs at
3, 6 and 9 knots

EFFECTS OF DOPPLER SHIFT IN SPREAD SPECTRUM ACQUISITION.

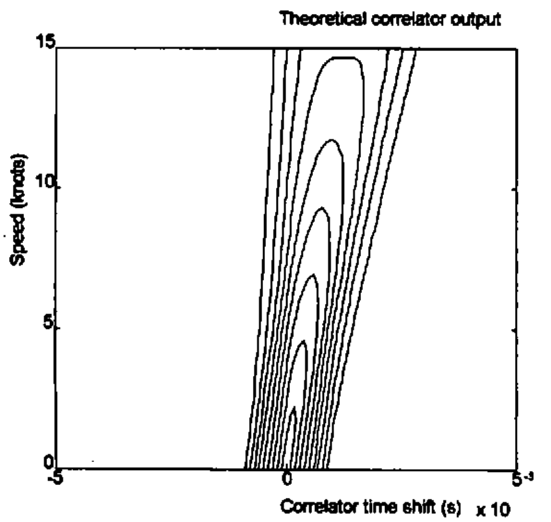

Figure 15 - Contour plot of theoretical ambiguity surface

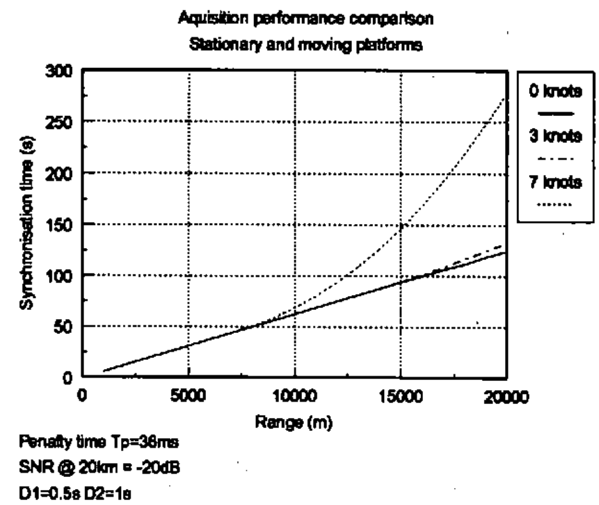

Figure 16 - Synchronisation performance at 0, 3 and 7 knots.

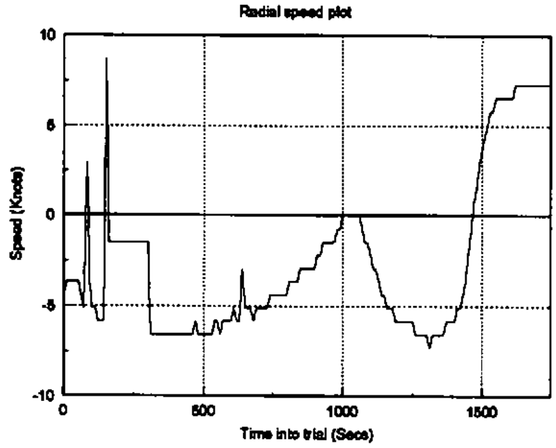

Figure 17 - Radial speed plot obtained from encoded signal